Hindawi Publishing Corporation
Journal of Chemistry
Volume 2016, Article ID 5620316, 6 pages
http://dx.doi.org/10.1155/2016/5620316

Research Article

Study on Low-Temperature Catalytic Dehydrogenation Reaction of Tail Chlorine by Pd/Al_2O_3

Hanhan Wang, Tingting Lu, Yuna Li, Bo Wu, Jianwei Xue, Fuxiang Li, and Zhiping Lv

College of Chemistry and Chemical Engineering, Taiyuan University of Technology, Taiyuan 030024, China

Correspondence should be addressed to Jianwei Xue; xuejianwei@tyut.edu.cn

Received 1 June 2016; Revised 26 September 2016; Accepted 18 October 2016

Academic Editor: Hossein Kazemian

The catalytic dehydrogenation reaction of tail chlorine by Pd was studied using a fixed-bed reactor at low temperature from 30 to 100°C. Different catalyst supports such as SiO_2 and Al_2O_3 were applied to prepare Pd catalysts by the incipient-wetness impregnation method. And the catalysts were characterized by XRD, FTIR, XPS, SEM, and N_2 adsorption-desorption. The catalyst Pd loading on both SiO_2 and Al_2O_3 had a catalytic effect on the dehydrogenation reaction, but the carrier Al_2O_3 was more superior. The hydrogen conversion and selectivity of hydrogen-oxygen reaction increased first and then decreased with Pd loading amount and temperature by using Pd/Al_2O_3 as catalysts, but the influence of temperature was limited when it was higher than 60°C. The hydrogen conversion was 97.38% and selectivity of hydrogen-oxygen reaction was 79% when the reaction temperature was at 60°C with 1 wt.% Pd/Al_2O_3.

1. Introduction

Chloralkali industry developed rapidly as a pillar industry in the inorganic chemical area. A large amount of chlorine-containing gas (tail chlorine), which contains hydrogen, nitrogen, oxygen, and other ingredients, is produced in the traditional production of chlorine in the electrolysis process. Considering the explosion risk of hydrogen, a part of the hydrogen must be removed to keep its content not higher than 4% by volume.

At the present stage, the typical treatment of tail chlorine is mainly by the combustion of a certain proportion of hydrogen and chlorine to synthesize the hydrochloric acid. However, the byproduct of hydrogen chloride would become excess and the cost of hydrogen chloride disposal by neutralization is high. Additionally, the shipment of this potentially hazardous waste is strictly limited. Thus, many researchers concentrated on the recovery of chlorine from hydrogen chloride by catalytic oxidation. Han et al. [1] made the conversion of hydrogen chloride to chlorine by catalytic oxidation in a two-zone circulating fluidized bed reactor at reaction temperature above 200°C. Feng et al. [2] prepared an efficient Cu-K-La/γ-Al_2O_3 catalyst for catalytic oxidation of chlorine from hydrogen chloride and the results showed a good catalytic performance and stability of conversion. Given that, the explosion problem of containing hydrogen in tail chlorine cannot be easily solved by combustion of hydrogen and chlorine to synthesize hydrochloric acid. The production of hydrogen chloride in the treatment of tail chlorine can also be reduced by other effective methods.

In 1957, Kulcsar and Kulcsar-Novakova developed a catalyst supported by activated carbon, which dehydrogenated the tail chlorine by catalyzing the reaction of hydrogen and chlorine to form hydrogen chloride [3]. Tanno [4] studied extensively the catalytic reaction conditions of hydrogen-chlorine reaction, which showed that higher temperature and lower gas flow rate made the performance of dehydrogenation better. Catalytic removal of hydrogen from electrolytic chlorine was studied by using charcoal, zeolite, and so forth at 20–300°C [5]. Pieters and Wenger [6] found that the concentration of hydrogen in a mixed gas could be reduced as low as ppm level by palladium catalyst loaded on Al_2O_3, or by catalysts $LaCl_3$, KCl, and CuCl doped on SiO_2. However, the way of removing hydrogen from tail chlorine by catalytic hydrogen-chlorine reaction has many disadvantages, such as high reaction temperature and short life of catalysts.

This paper aimed to research the catalytic performance of palladium on hydrogen-oxygen reaction, which could safely

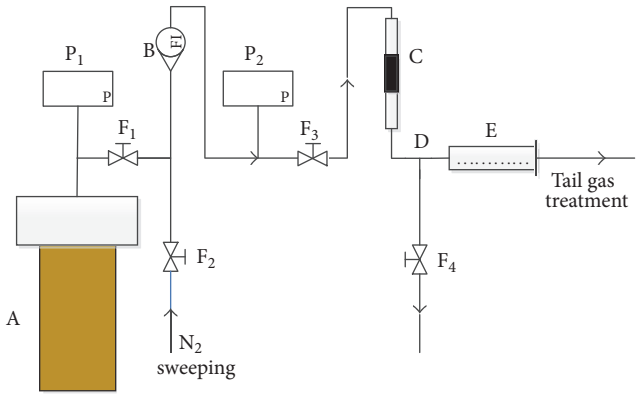

Figure 1: The device for removing hydrogen from the tail chlorine. (A) Gas tank, (B) rotor flowmeter, (C) fixed-bed reactor, (D) sampling device, and (E) water adsorption device. F_1, F_2, F_3, and F_4 represent valves, and P_1 and P_2 represent vacuum gauges.

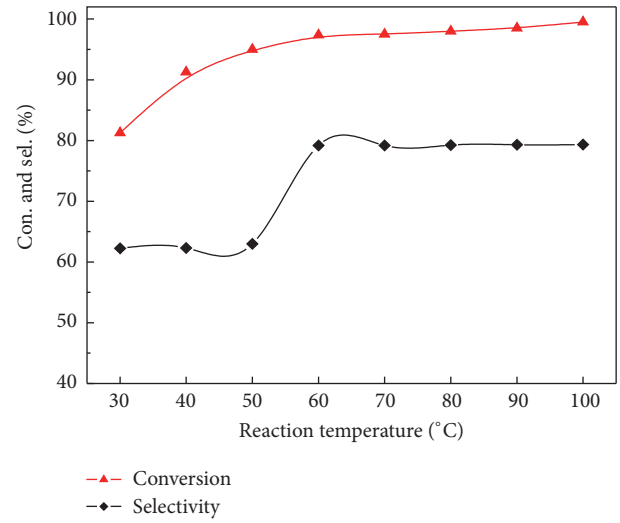

Figure 2: Hydrogen conversion and selectivity of hydrogen-oxygen reaction of Pd/Al_2O_3 at different reaction temperatures.

remove hydrogen from trail chlorine at low temperature and increase the economic value of tail chlorine.

2. Materials and Methods

2.1. Catalyst Preparation. The supported palladium catalysts were prepared by incipient-wetness impregnation method. 1.0 g supports as γ-Al_2O_3 or SiO_2 powder were impregnated into the hydrochloric acid solution of palladium chloride at room temperature for 24 h and then dried in a drying oven for 6 h. Finally, the dried catalysts were calcined in muffle furnace at 500°C and activated in hydrogen atmosphere at 250°C for 4.5 h. The freshly prepared Pd/SiO_2 and Pd/Al_2O_3 catalysts were stored in a dry and sealed plastic bag before use.

2.2. Catalytic Dehydrogenation Reaction of Tail Chlorine. The catalytic performance was evaluated in a fixed-bed reactor system as shown in Figure 1. A certain amount of catalysts was loaded in the fixed-bed reactor. The simulated gas mixture that was composed of Cl_2, O_2, H_2, and N_2 according to the composition of industrial tail chlorine was introduced into the reactor at a specific reaction temperature. The entire gas line was purged with nitrogen before introducing the simulated gas mixture. The products of catalytic dehydrogenation reaction were analyzed periodically. Water was absorbed by P_2O_5 stored in an adsorption device, which was weighed at set intervals. The weight increment of the water adsorption device was the water formed during that time interval. The produced hydrochloric acid was measured by titration in saturated NaCl solution.

2.3. Catalyst Characterization. Scanning electron microscopy (SEM) was performed on a Philips XL30 working at 20 kV. The specific surface area and distribution of pore size were measured by N_2 adsorption-desorption method at −196°C with a Micromeritics (ASAP 2020) instrument. X-ray diffraction (XRD) patterns were recorded on a Rigaku-DMax (2500PC) with Cu Kα radiation in the 2θ range from 10° to 90° with 0.02°/min. X-ray photoelectron spectroscopy (XPS) measurements were performed on a Physical Electronics (PHI 1600) spectrometer using Mg Kα radiation and photon energies of 1253.6 eV.

3. Results and Discussion

3.1. The Influence of Reaction Temperature on Catalytic Dehydrogenation Reaction. As shown in Figure 2, the hydrogen conversion increased with increasing temperature from 30 to 60°C, while the increase was not obvious when the temperature exceeded 60°C. The hydrogen conversion rose from 91.25% at 30°C to 97.38% at 60°C; with further increase of temperature to 70°C, it only reached 99.5%. In general, the selectivity of hydrogen-oxygen reaction increased with increasing temperature, while the variation trend could be separated into three stages. At low temperature from 30 to 50°C, the selectivity almost kept constant as 62%, and then it dramatically increased up to 79.19% at 60°C; after that, the selectivity became stable again at the high temperature range from 60 to 100°C. Thus, the reaction temperature of the catalytic dehydrogenation was 60°C, which provided high selectivity of the aimed reaction with low energy consumption.

3.2. The Influence of Support on the Performance of Catalytic Dehydrogenation Reaction. As shown in Figure 3, the dehydrogenation catalyzed by Pd/Al_2O_3 kept higher hydrogen conversion than that catalyzed by Pd/SiO_2 during the whole reaction process, which was attributed to the different type of surface acid sites provided by Al_2O_3 and SiO_2. It has been reported [7] that the L surface acid site was beneficial to hydrogen adsorption by Pd. The surface of Al_2O_3 had mainly L acid, but the surface of SiO_2 had mostly B acid, and thus Pd/Al_2O_3 showed better catalytic performance in hydrogen conversion. The selectivity of hydrogen-oxygen reaction of Pd/SiO_2 was slightly higher than that of Pd/Al_2O_3 as illustrated in Figure 4. Overall, the catalyst of Pd/Al_2O_3 had better performance for catalyzing the dehydrogenation.

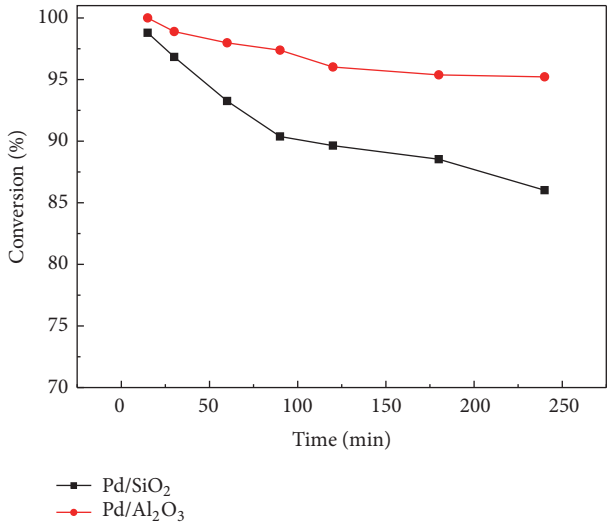

Figure 3: Hydrogen conversion in catalytic dehydrogenation of Pd/SiO_2 and Pd/Al_2O_3.

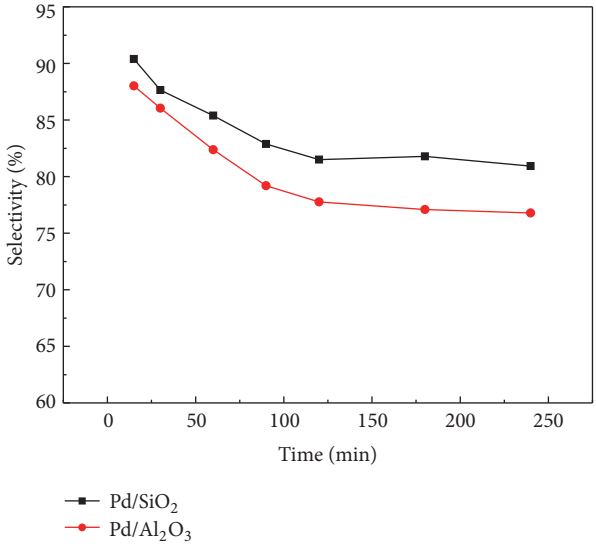

Figure 4: Selectivity of hydrogen-oxygen reaction in the catalytic reaction of Pd/SiO_2 and Pd/Al_2O_3.

3.3. The Influence of Pd Loading on Performance of Catalytic Dehydrogenation Reaction. The effect of Pd loading amount on the performance of Pd/Al_2O_3 in catalytic dehydrogenation reaction was assessed at 60°C as shown in Figures 5 and 6. Pd/Al_2O_3 with different Pd loading amount maintained the catalytic activity during the whole reaction process. The performance of Pd/Al_2O_3 was improved by increasing the Pd loading amount from 0.4 to 1.0% wt.; however, the continuous increase of Pd loading was detrimental. Thus, the optimal Pd loading amount was 1.0% wt. With the increasing concentration of $PdCl_4^{2-}$ in the impregnate solution, the active ingredient content of catalyst increased and the crystallinity of palladium increased as well, resulting in better performance of Pd/Al_2O_3. However, the too high Pd loading would cause the increase of grain and the decrease of particle dispersion,

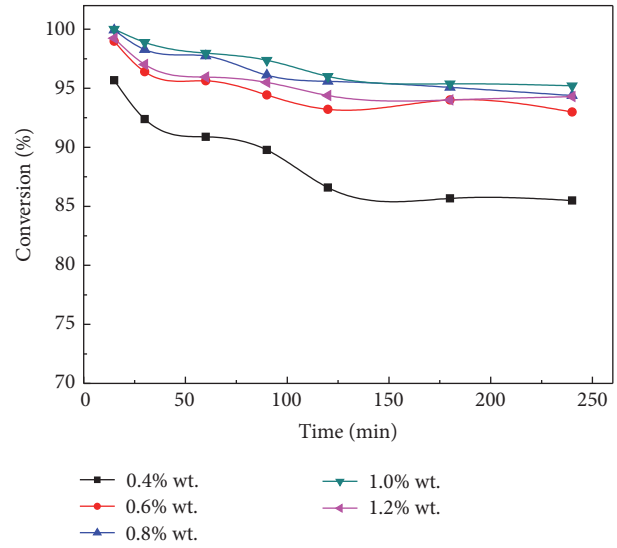

Figure 5: The hydrogen conversion of Pd/Al_2O_3 in catalytic dehydrogenation reaction.

which reduced the effective contact area between the active ingredient and the reaction gas, resulting in poor Pd/Al_2O_3 performance. Dispersion of solid particles is a key factor affecting the optimal effects of the catalyst [8].

3.4. The Effect of Dehydrogenation Reaction on Pd/Al_2O_3 Catalyst. The characteristics of Pd/Al_2O_3 could be modified during the dehydrogenation reaction. The analyses of XRD, FTIR, XPS, and N_2 adsorption-desorption were examined to investigate the modification of Pd/Al_2O_3 properties.

3.4.1. The XRD Patterns of Different Loadings of Pd/Al_2O_3. The XRD analysis of Pd/Al_2O_3 of different Pd loading amounts before reaction was illustrated in Figure 7. The characteristic peaks corresponding to metallic Pd presented at about $2\theta = 40^\circ$, 45°, and 68°. The diffraction peaks of metallic Pd could not be observed with the loading amount from 0.4% to 0.6% due to the high dispersion of a small amount of Pd particles [9]. With increasing loading of Pd, the characteristic peaks of Pd became obvious and sharper at 1.2% wt., which indicated that the crystallization degree obviously increased. According to the previous studies [10], the high crystallization degree would cause the growth of grain and further enhance the degree of aggregation, which inhibited the activity of the catalyst. This was consistent with the experimental result in this study.

3.4.2. The XRD Patterns of Pd/Al_2O_3 before and after Reaction. Before reaction, the characteristic diffraction peaks of γ-Al_2O_3 were obtained at about 36°, 45°, and 68°, and the characteristic diffraction peaks of Pd were obtained at 40° and 47° as shown in Figure 8(a). After 240 min dehydrogenation reaction, the position and intensity of characteristic peaks of γ-Al_2O_3 and Pd did not change, as shown in Figure 8(b). This indicated that the catalyst of Pd/Al_2O_3 had good stability.

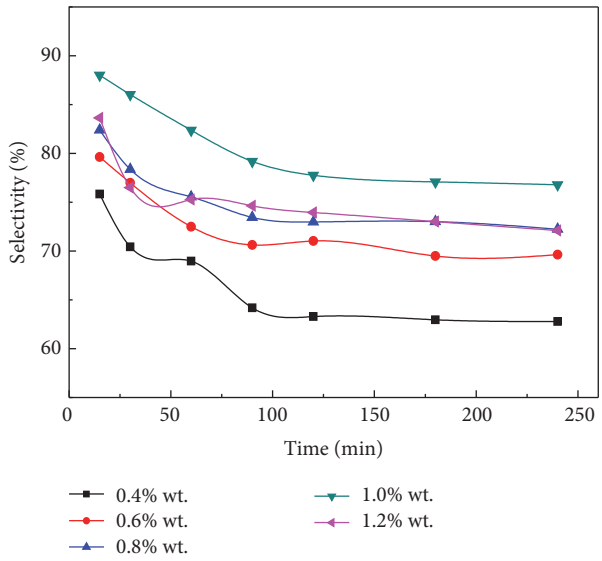

Figure 6: The hydrogen-oxygen selectivity of Pd/Al_2O_3 in catalytic dehydrogenation reaction.

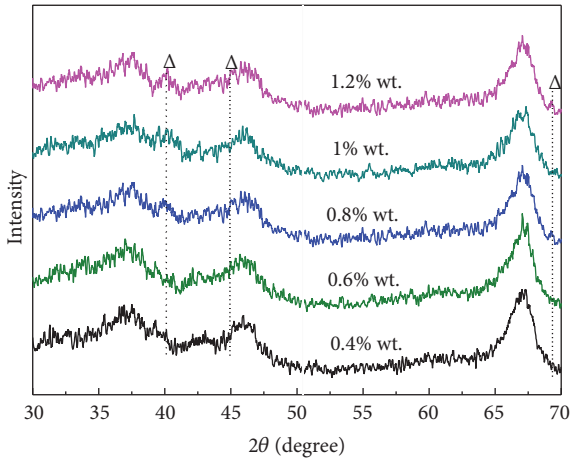

Figure 7: The XRD patterns of different loadings of Pd/Al_2O_3.

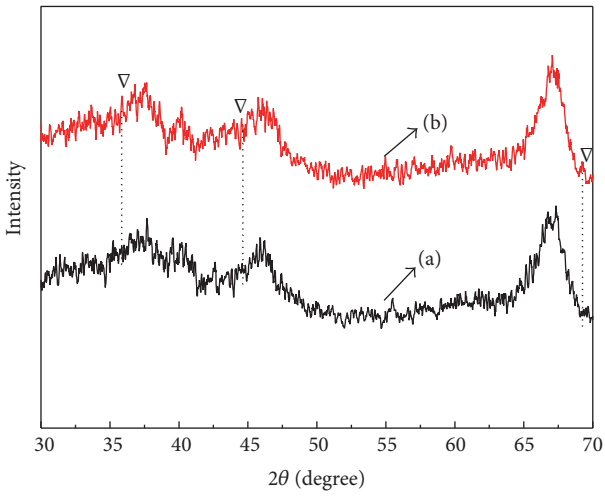

Figure 8: The XRD patterns of 1% Pd/Al_2O_3 before and after reaction. (a) 1% Pd/Al_2O_3; (b) 1% Pd/Al_2O_3 after reaction.

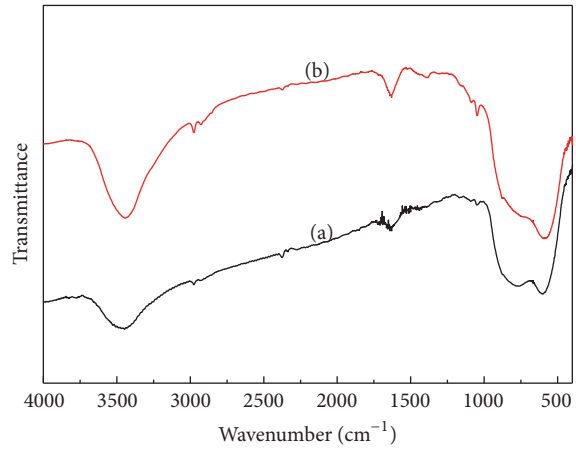

Figure 9: The FTIR spectra of 1% Pd/Al_2O_3 before and after reaction. (a) 1% Pd/Al_2O_3; (b) 1% Pd/Al_2O_3 after reaction.

3.4.3. The FTIR Spectra of Pd/Al_2O_3. As shown in Figure 9, the absorption peak in 620 cm^{-1} was the six-coordinated characteristic absorption peak of Al^{3+} and the strong absorption peak in 880 cm^{-1} could be attributed to the four-coordinate of Al-O vibration. The relatively weak peak that appeared in 1650 cm^{-1} could be attributed to the bending vibration of H-OH bond which was relative to the existence of free water. The absorption peak in 3450 cm^{-1} might be caused by the stretching vibration of the water absorption by carriers or the absorption peak of –OH [11]. After catalytic dehydrogenation reaction, the characteristic absorption peaks in 400 cm^{-1}~900 cm^{-1} still existed and the intensity of characteristic absorption peaks in 1650 cm^{-1} and 3450 cm^{-1} increased because of the absorption of the water generated in the reaction by γ-Al_2O_3.

3.4.4. The XPS Spectra of Pd/Al_2O_3. According to XPS analysis shown in Figure 10, the standard binding energies of $Pd^0 3d_{5/2}$ and $Pd^0 3d_{3/2}$ were at 335.2 eV and 340.5 eV, respectively. However, the binding energies of $Pd^0 3d_{5/2}$ and $Pd^0 3d_{3/2}$ were at 337.23 eV and 342.51 eV when Pd was loaded on γ-Al_2O_3, which indicated that the combining force of Pd and γ-Al_2O_3 was stronger, which was consistent with the conclusion obtained by Ihm et al. [12]. After the catalytic dehydrogenation reaction, the binding energies of $Pd^0 3d_{5/2}$ and $Pd^0 3d_{3/2}$ moved to 337.33 eV and 342.77 eV, whereas the intensity and area of peaks had a certain degree of decline. The result was attributed to the oxidation of Pd^0 by O_2 or Cl_2 to Pd^{2+}, leading to positive displacement of binding energy. Overall, Pd^0 still had a high percentage after reaction and the catalyst characteristics remained relatively stable.

3.4.5. N_2 Adsorption-Desorption and Pore Diameter of Pd/Al_2O_3. The N_2 adsorption-desorption isotherms curves of Al_2O_3 and 1% Pd/Al_2O_3 were illustrated in Figure 11. The curves belonged to type IV isotherm [13] curve and the shape of the hysteresis loop was H3 type. The nitrogen adsorption curves became higher in high P/P_0, corresponding to the

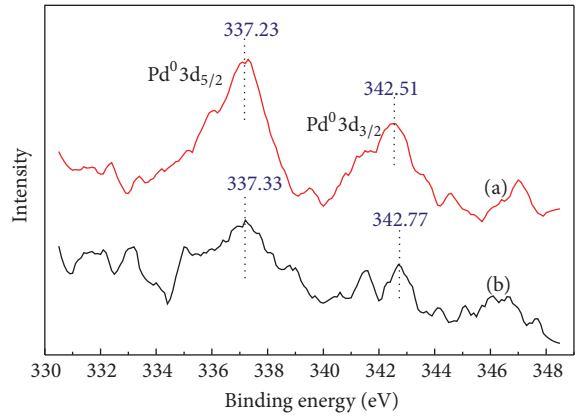

Figure 10: The XPS spectra of 1% Pd/Al_2O_3 before and after reaction. (a) 1% Pd/Al_2O_3; (b) 1% Pd/Al_2O_3 after reaction.

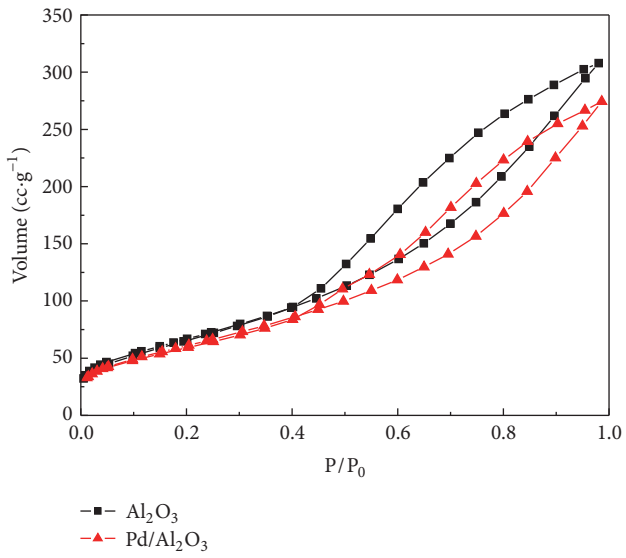

Figure 11: The N_2 adsorption-desorption isotherms of Al_2O_3 and 1% Pd/Al_2O_3.

existence of parallel tubular capillary and slit-shaped pores [14]. The shape of N_2 adsorption-desorption isotherm of Al_2O_3 was not changed obviously by loading with Pd, which only had a slight decrease in the hysteresis loop area, which was the phenomenon of capillary condensation inside the carrier.

Figure 12 showed the pore diameter of Al_2O_3 and 1% Pd/Al_2O_3, which were analyzed by the BJH model. The pore distribution of alumina was mainly at about 5 nm before loading. However, there was a new peak at about 7 nm after loading by Pd, which was attributed to the minor damage of the pore structure by the immersion of acid. As could be seen from Table 1, the average pore diameters of Al_2O_3 and 1% Pd/Al_2O_3 were almost the same, but the specific surface area and total pore volume were reduced to a certain extent after loading, which indicated that the active ingredient of palladium was mainly formed at the external surface and

Table 1: Specific surface area, total pore volume, and pore diameter of Al_2O_3 and 1% Pd/Al_2O_3.

Sample	Specific surface area ($m^2 \cdot g^{-1}$)	Total pore volume ($cm^3 \cdot g^{-1}$)	Average pore diameter (nm)
Al_2O_3	258.133	0.4761	3.854
Pd/Al_2O_3	235.262	0.4243	3.809

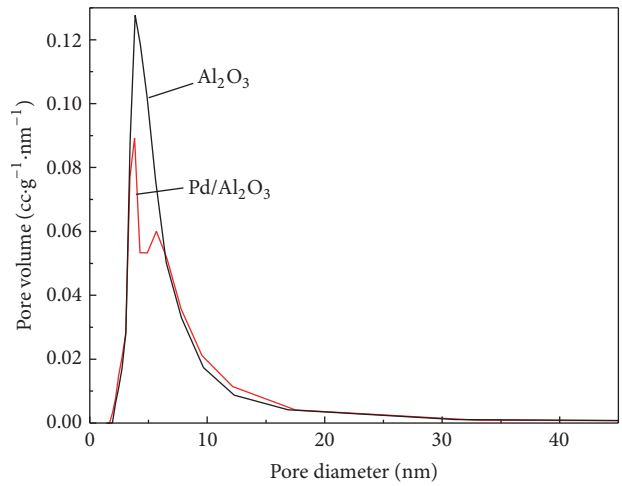

Figure 12: The pore diameter of Al_2O_3 and 1% Pd/Al_2O_3.

the wall of pores close to the external surface of the support particle.

3.4.6. The SEM Analysis of the Influence of Pd Loading on Al_2O_3. Further evidence of the in-framework metal Pd loading on Al_2O_3 was provided by SEM analyses, as shown in Figures 13–15. There was a comparison of Al_2O_3 and Pd/Al_2O_3 in Figures 13 and 14, and Figure 15 shows the partial enlarged detail of Figure 14. Obviously, it could be seen from Figures 14-15 that metal Pd uniformly loaded on Al_2O_3 was noted in the SEM. These figures also showed that the skeleton structure of Al_2O_3 was not changed, which indicated that the catalyst Pd/Al_2O_3 structure was stable.

4. Conclusion

(1) Pd/Al_2O_3 and Pd/SiO_2 both had a catalytic effect on the dehydrogenation reaction at low temperature.

(2) With the increase of Pd loading and reaction temperature, the hydrogen conversion and selectivity of Pd/Al_2O_3 in catalytic dehydrogenation reaction increased firstly and then decreased, but the impact of reaction temperature on the catalytic performance is not obvious after 60°C.

(3) When Pd loading is 1% and the reaction temperature is 60°C, hydrogen conversion and oxygen-hydrogen selectivity of Pd/Al_2O_3 are at 97.38% and 75%. The performance of Pd/Al_2O_3 is better than Pd/SiO_2.

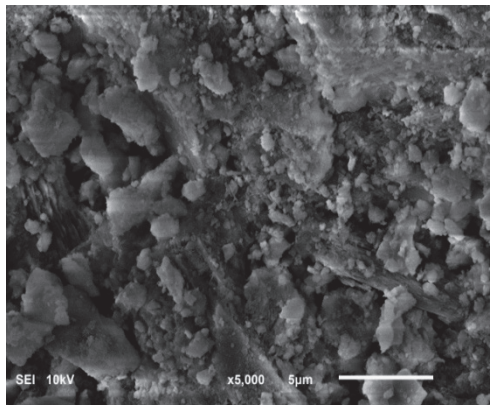

Figure 13: SEM images of Al_2O_3.

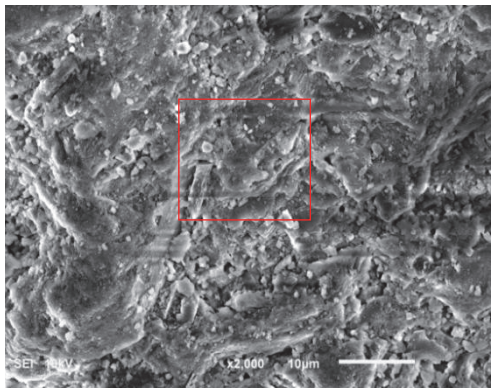

Figure 14: SEM images of Pd/Al_2O_3.

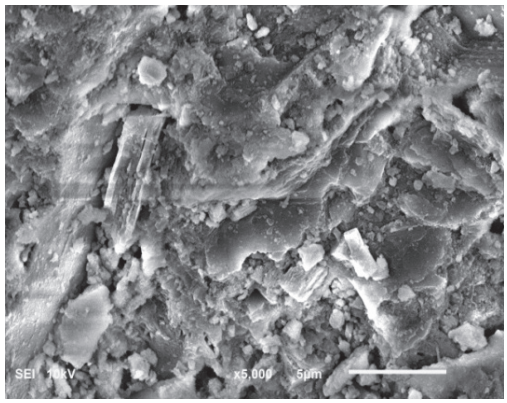

Figure 15: SEM images of Pd/Al_2O_3.

Competing Interests

The authors declare that they have no competing interests.

References

[1] M. Han, P. Chang, G. Hu, Z. Chen, D. Wang, and F. Wei, "Conversion of hydrogen chloride to chlorine by catalytic oxidation in a two-zone circulating fluidized bed reactor," *Chemical Engineering and Processing: Process Intensification*, vol. 50, no. 7, pp. 593–598, 2011.

[2] K. Feng, C. Li, Y. Guo et al., "An efficient Cu-K-La/γ-Al_2O_3 catalyst for catalytic oxidation of hydrogen chloride to chlorine," *Applied Catalysis B: Environmental*, vol. 164, pp. 483–487, 2015.

[3] G. J. Kulcsar and M. Kulcsar-Novakova, "The slow combustion of hydrogen in the chlorine resulting from electrolysis in order to avoid explosions. II. The study of the slow combustion of hydrogen in chlorine in the presence of active carbon in order to determine the technical characteristics of the reaction," *Studii si Cercetari de Chimie*, vol. 8, pp. 221–230, 1957.

[4] H. Tanno, "Removal of hydrogen in chlorine-containing gas," Patent JP37010417, 1962.

[5] A. A. Krasheninnikova, A. S. Kulyasova, and A. A. Furman, "Catalytic method for removing hydrogen from electrolytic chlorine," *Khimicheskaya Promyshlennost*, no. 5, pp. 364–365, 1975.

[6] W. J. M. Pieters and F. Wenger, "Removal of low concentrations of hydrogen from chlorine gas," Patent, US4224293, 1980.

[7] R.-X. Jiang, Z.-K. Xie, C.-F. Zhang, Q.-L. Chen, and J.-H. Sun, "Effects of promoters on the properties of Pd/Al_2O_3 catalyst in gas-phase amination," *Acta Petrolei Sinica (Petroleum Processing Section)*, vol. 20, no. 2, pp. 13–20, 2004.

[8] Z. P. Cherkezova-Zheleva, M. G. Shopska, J. B. Krstić, D. M. Jovanović, I. G. Mitov, and G. B. Kadinov, "A study of the dispersity of iron oxide and iron oxide-noble metal (Me = Pd, Pt) supported systems," *Russian Journal of Physical Chemistry A*, vol. 81, no. 9, pp. 1471–1476, 2007.

[9] M.-Y. Kim, E. A. Kyriakidou, J.-S. Choi et al., "Enhancing low-temperature activity and durability of Pd-based diesel oxidation catalysts using ZrO_2 supports," *Applied Catalysis B: Environmental*, vol. 187, pp. 181–194, 2016.

[10] M. Wen, Z. Qu, X. Zhang et al., "Low-temperature CO oxidation over Ag/SiO_2 catalysts," *Sciencepaper Online*, vol. 4, no. 5, pp. 367–372, 2009.

[11] R. Khoshbin, M. Haghighi, and N. Asgari, "Direct synthesis of dimethyl ether on the admixed nanocatalystsof CuO-ZnO-Al_2O_3 and HNO_3-modified clinoptilolite at high pressures: surface properties and catalytic performance," *Materials Research Bulletin*, vol. 48, no. 2, pp. 767–777, 2013.

[12] S.-K. Ihm, Y.-D. Jun, D.-C. Kim, and K.-E. Jeong, "Low-temperature deactivation and oxidation state of Pd/γ-Al_2O_3 catalysts for total oxidation of n-hexane," *Catalysis Today*, vol. 93–95, pp. 149–154, 2004.

[13] S. J. Gregg and K. S. W. Sing, *Adsorption, Surface Area and Porosity*, Academic Press, New York, NY, USA, 1982.

[14] R. Yang, Y. Lin, J. Feng, D. G. Evans, and D. Li, "Preparation of supported Pd/Al2O3 catalysts by ultrasonic impregnation and their catalytic performance for anthraquinone hydrogenation," *Chinese Journal of Catalysis*, vol. 27, no. 4, pp. 304–308, 2006.